Low-frequency raman spectra and phase transitions in perovskite-type layer compounds. (CH3NH3)2MnCl4 and (CH3NH3)CdCl4

ARTICLE *in* PHYSICA STATUS SOLIDI (A) · MAY 1977

Impact Factor: 1.21 · DOI: 10.1002/pssa.2210410133

3 AUTHORS, INCLUDING:

Michel Couzi
University of Bordeaux
234 PUBLICATIONS **3,611** CITATIONS

phys. stat. sol. (a) **41**, 271 (1977)

Subject classification: 1.2; 6; 20.1; 22.9

Laboratoire de Spectroscopie Infrarouge, associé au C.N.R.S., Université de Bordeaux I, Talence[1]) *(a) and Laboratoire de Recherches sur la Réactivité des Solides, associé au C.N.R.S., Faculté des Sciences Mirande, Dijon*[2]) *(b)*

Low-Frequency Raman Spectra and Phase Transitions in Perovskite-Type Layer Compounds

$(CH_3NH_3)_2MnCl_4$ and $(CH_3NH_3)_2CdCl_4$

By

M. Couzi (a), A. Daoud[3]) (b), and R. Perret (b)

The low-frequency (0 to 500 cm^{-1}) Raman spectra are recorded at different temperatures between 40 and 413 K through the different structural modifications: $P2_1/c \leftrightarrow P4_2/ncm \leftrightarrow Cmca \leftrightarrow \leftrightarrow I4/mmm$. The results agree with previous NMR data and show that the three higher-temperature tetragonal and orthorhombic phases exhibit specific disorder with respect to the orientation of the methylammonium cation while the monoclinic low-temperature modification is ordered. A soft-mode behaviour is observed in the intermediate $P4_2/ncm$ and Cmca phases, associated with the high-temperature second-order $Cmca \leftrightarrow I4/mmm$ transition. A discussion of the unusual phase sequence in these materials is tentatively given, in view of previously proposed mechanisms for the phase transitions.

Les spectres Raman de basse fréquence (0 à 500 cm^{-1}) ont été enregistrés à différentes températures comprises entre 40 et 413 K, dans les différentes phases cristallines: $P2_1/c \leftrightarrow P4_2/ncm \leftrightarrow \leftrightarrow Cmca \leftrightarrow I4/mmm$. Les résultats sont en accord avec des données RMN antérieures et montrent que les trois phases de plus haute température (tétragonales et orthorhombique) présentent un désordre spécifique dans l'orientation des cations méthylammonium, alors que la phase monoclinique de basse température est ordonnée. Un comportement de mode mou est associé à la transition du 2e ordre $Cmca \leftrightarrow I4/mmm$ de haute température observé dans les phases intermédiaires $P4_2/ncm$ et Cmca. Une discussion de la séquence de phase inhabituelle de ces matériaux est faite sur la base des mécanismes de transitions de phase proposés antérieurement.

1. Introduction

The compounds $(C_nH_{2n+1}NH_3)_2MCl_4$, with M = Mn, Cd and $n = 1, 2, \ldots$, crystallize in a perovskite-type layer structure [1 to 6] consisting of nearly isolated layers of corner-sharing MCl_6 octahedra. The cavities between octahedra contain the NH_3 groups of the alkylammonium ions, which form hydrogen bonds with the chlorine atoms of the layer. Interlayer bonding is only achieved by van der Waals forces between the ends of the carbon chains.

The methyl compounds ($n = 1$) of the manganese and the cadmium family exhibit an unusual phase sequence [2 to 6], whith transition temperatures given below:

Mn	394 K	257 K	94 K
Cd	484 K	279 K	163 K

$I4/mmm \leftrightarrow$	$Cmca \leftrightarrow$	$P4_2/ncm \leftrightarrow$	$P2_1/c$
$(Z = 2)$	$(Z = 4)$	$(Z = 4)$	$(Z = 2)$
THT	ORT	TLT	MLT.

[1]) 351, cours de la Libération, 33405 Talence Cedex, France.

[2]) 21000 Dijon, France.

[3]) Present address: Faculté des Sciences et Techniques Sfax, Tunisia.

Recently, this sequence of structural phase transitions was extensively investigated by means of X-rays [5, 6] and neutron diffraction [2 to 4], optical birefringence [2], as well as by means of the NMR and NQR techniques [7 to 10], and by dielectric [11], calorimetric [12, 13], Raman and infrared measurements [14 to 18]. From these studies, it was clearly established that in both compounds, the high-temperature phase transition is continuous (second order) while the other two transitions have a strong first-order character. It is also clear the phase transformations are governed by changes in the motion of the CH_3NH_3 groups, as well as in the hydrogen bond scheme. Furthermore, for all phases but the monoclinic one, the methylammonium groups are in a specifically disordered state [6] of a dynamic nature [7 to 10].

A group-theoretical analysis has shown that the soft mode associated with the second-order transition between the tetragonal high-temperature (THT) and the orthorhombic room-temperature (ORT) phases transforms according to the $\tau_5(B_{3g})$ representation at point $X(\frac{1}{2}, \frac{1}{2}, 0)$ of the tetragonal Brillouin zone boundary, and becomes a totally symmetric (A_g) zone centre mode in the ORT phase [19]. Furthermore, preliminary Raman studies on $(CH_3NH_3)_2MnCl_4$ [17, 18] and $(CH_3NH_3)_2CdCl_4$ [18] revealed the existence of a broad low-frequency feature in the ORT and the tetragonal low-temperature (TLT) phases, which was tentatively assigned to this soft mode [17].

The structural phase transformations of these perovskite-type layer compounds lead to many interesting questions from a lattice dynamical point of view. Thus, we have recorded the low-frequency Raman spectra of $(CH_3NH_3)_2MnCl_4$ and $(CH_3NH_3)_2 \cdot CdCl_4$ through their different structural modifications. In this paper we shall give a preliminary and qualitative analysis of these spectra, based upon the recently proposed mechanism for the phase sequence [5, 6, 8 to 10].

2. Phase Transitions and Group Theory

In the THT phase, where $Z = 1$ in the primitive unit cell, the $CH_3NH_3^+$ groups are attached by N–H ... Cl hydrogen bonds such that two N–H bonds lead to equatorial Cl(1) atoms of the chlorine octahedra, and one to an axial Cl(2) site [3, 6]. This leads to a tilting of the C–N direction by an angle of about 20° with respect to the fourfold axis. There are at least four different orientations of the CN bond with equal occupation probabilities, $W_1 = W_2 = W_3 = W_4 = \frac{1}{4}$, so that the time-averaged configuration of the $CH_3NH_3^+$ cation has the required fourfold site symmetry. They are related to each other by a jumpwise rotation by $\pm$ 90° of the CN bond on a conical surface around the unique axis, and are associated to four energetically equivalent tilted configurations of the MCl_6 octahedra [3].

The ORT phase (space group Cmca and $Z = 2$ in the primitive unit cell) is related to the THT phase by a doubling of the unit cell in the plane of the layer [3, 5]. From X-rays and neutron data this phase is seen as a "frozen" moment picture of the THT phase, where no disorder remains [3]. However, a complete freezing of the tumbling mode of the $CH_3NH_3^+$ ions in the favoured potential well at the phase transition would cause a flip in the time-averaged CN direction about 20° and does not agree with a second-order phase transition; furthermore, the transition entropy of 0.03 cal/mol K in $(CH_3NH_3)_2MnCl_4$ [14] is too small for a complete freezing of the tumbling mode [9]. Indeed, NMR and NQR investigations [7 to 10] indicate that the tumbling mode exists down to the first-order TLT $\leftrightarrow$ MLT (monoclinic low-temperature) transition. Thus, in the ORT phase, one of the four potential wells becomes favoured ($W_1 > W_2 = W_4 > W_3$) caused by a biasing of the tumbling mode, so that the time-averaged CN direction moves continuously out of the cone axis when going through the second-order transition [9].

In the TLT phase, where $Z = 4$ in the primitive unit cell, the identity period now corresponds to two interlayer distances [4, 5]. Neutron diffraction data on $(CH_3NH_3)_2 \cdot MnCl_4$ indicate that the $CH_3NH_3^+$ group has not the same configuration as in the ORT and THT phases, i.e. one N–H bond leads to equatorial Cl(1) atom and two N–H bonds to axial Cl(2) sites [4]. In contrast, X-ray results on $(CH_3NH_3)_2CdCl_4$ [5] have been interpreted in the TLT phase by the existence of five hydrogen positions. As pointed out by Seliger et al. [10] these five hydrogen positions can be understood by a superposition of two $CH_3NH_3^+$ orientations according to the "orthorhombic" hydrogen bond scheme. Following this model (i), at the ORT $\leftrightarrow$ TLT transition, there is a sudden change of the occupation probabilities to $W_1 = W_4 = \frac{1}{2}$, $W_2 = W_3 = 0$ [10].

The primitive unit cell of the MLT phase is $P2_1/c$ with two formula units [6]; in this phase the identity period again corresponds to one interlayer distance. The $CH_3NH_3^+$ cations are ordered in one configuration where one N–H ... Cl bond leads to equatorial Cl(1) and two N–H bonds to axial Cl(2) sites [6] (i.e. it is the configuration deduced in the TLT phase from neutron diffraction data [4]). In this "monoclinic" configuration, there are again four possible orientations for the $CH_3NH_3^+$ group, but only one is occupied, due to strong lattice distortions [6]. According to NMR data [8, 10] the tumbling mode is completely frozen in, whereas the hindered rotations of the CH_3 and NH_3 groups still exist in this phase.

Small deviations of the above-described model (i) for the phase sequence were also developed [10]. In particular, it was considered [5, 10] that both the "orthorhombic" and the "monoclinic" configurations of $CH_3NH_3^+$ could exist in the TLT phase (model (ii)). Also, the indication of a splitting of each $CH_3NH_3^+$ potential well into two minima in the THT phase [3] leads to a very similar jumpwise reorientational model (iii) with eight potential wells [10].

The group-theoretical analysis of the lattice vibrations in the THT and ORT phases made by Petzelt [19] is summarized in Table 1. We have also indicated our results for the TLT and MLT phases. It is important to notice that a rigorous factor-group analysis cannot be made in disordered crystals, because of the breakdown of the lattice translational symmetry. The results given in Table 1 are obtained by considering the time-averaged configuration of the $CH_3NH_3^+$ ions in the disordered THT, ORT, and TLT phases. Also, the description of the lattice modes in terms of $(MCl_4)_n^{2n-}$ vibrations and of librations and translatory vibrations of the $CH_3NH_3^+$ groups (Table 1) is convenient but not rigorous. In fact, the validity of this description can only be established from a complete analysis of the spectra.

3. Experimental

Faint pink $(CH_3NH_3)_2MnCl_4$ and colourless $(CH_3NH_3)_2CdCl_4$ crystals were prepared at room temperature as described earlier [18]. Platelet-shaped single crystals about $10 \times 10 \times 2$ mm^3 were used for our Raman scattering measurements.

The Raman spectra in the low-frequency region (0 to 500 cm^{-1}) were recorded on a CODERG T800 triple monochromator instrument, coupled with a Spectra Physics argon ion laser model 171; the 5145 and 4880 Å emission lines were used. Detection was made with a photomultiplier EMI 9558 A with dc amplification.

A CODERG nitrogen continuous-flow cryostat was used to keep the samples at different temperatures between 80 and 300 K. Some spectra were recorded down to 40 K, using a CRYODYNE model 20 liquid helium refrigerator equiped with the sample holder modification described in [20]. The spectra at high temperatures up to 420 K were obtained with a small heating unit. In all cases, the temperature control monitored by a thermocouple was better than $\pm$ 0.5 K. The determination of the

Table 1

Factor-group analysis of the lattice vibrations of $(CH_3NH_3)_2MCl_4$ compounds in their different structural modifications

symmetry	$(MCl_4)_n^{2n-}$	$CH_3NH_3^+$		activity
		libr.	trans.	
THT phase — I4/mmm $\equiv D_{4h}^{17}$ ($Z = 1$)				
A_{1g}	1	0	1	Raman ($\alpha_{xx} + \alpha_{yy}$, α_{zz})
A_{2g}	0	1	0	inactive
B_{1g}	0	0	0	Raman ($\alpha_{xx} - \alpha_{yy}$)
B_{2g}	0	0	0	Raman (α_{xy})
E_g	1	1	1	Raman (α_{xz}, α_{yz})
A_{1u}	0	1	0	inactive
A_{2u}	2	0	1	IR ($\boldsymbol{E} \parallel \boldsymbol{z}$)
B_{1u}	0	0	0	inactive
B_{2u}	1	0	0	inactive
E_u	3	1	1	IR ($\boldsymbol{E} \parallel \boldsymbol{x}, \boldsymbol{y}$)
ORT phase — Cmca $\equiv D_{2h}^{18}$ ($Z = 2$)				
A_g	3	1	2	Raman (α_{xx}, α_{yy}, a_{zz})
B_{1g}	3	2	1	Raman (α_{xy})
B_{2g}	2	2	1	Raman (α_{xz})
B_{3g}	4	1	2	Raman (α_{yz})
A_u	3	2	1	inactive
B_{1u}	5	1	2	IR ($\boldsymbol{E} \parallel \boldsymbol{z}$)
B_{2u}	4	1	2	IR ($\boldsymbol{E} \parallel \boldsymbol{y}$)
B_{3u}	3	2	1	IR ($\boldsymbol{E} \parallel \boldsymbol{x}$)
TLT phase — $P4_2/ncm \equiv D_{4h}^{16}$ ($Z = 4$)				
A_{1g}	3	1	2	Raman ($\alpha_{xx} + \alpha_{yy}$, α_{zz})
A_{2g}	2	2	1	inactive
B_{1g}	2	2	1	Raman ($\alpha_{xx} - \alpha_{yy}$)
B_{2g}	3	1	2	Raman (α_{xy})
E_g	7	3	3	Raman (α_{xz}, α_{yz})
A_{1u}	2	2	1	inactive
A_{2u}	5	1	2	IR ($\boldsymbol{E} \parallel \boldsymbol{z}$)
B_{1u}	6	1	2	inactive
B_{2u}	2	2	1	inactive
E_u	9	3	3	IR ($\boldsymbol{E} \parallel \boldsymbol{x}, \boldsymbol{y}$)
MLT phase — $P2_1/c \equiv C_{2h}^5$ ($Z = 2$)				
A_g	6	3	3	Raman (α_{xx}, α_{yy}, α_{zz}, α_{xz})
B_g	6	3	3	Raman (α_{xy}, α_{yz})
A_u	8	3	3	IR ($\boldsymbol{E} \parallel \boldsymbol{y}$)
B_u	7	3	3	IR ($\boldsymbol{E} \parallel \boldsymbol{z}, \boldsymbol{x}$)

absolute temperature performed by the measurement of the Stokes/anti-Stokes intensity ratio of low-frequency Raman lines, indicated always higher temperatures than that given by the thermocouple disposed on the sample holder due to a local heating of the sample by the laser beam. In the case of the lightly coloured $(CH_3NH_3)_2 \cdot MnCl_4$ crystals this difference could reach 20 K for a sample holder temperature of about 80 K.

4. Results

We have recorded the Raman spectra of $(CH_3NH_3)_2MnCl_4$ and $(CH_3NH_3)_2CdCl_4$ single crystals through their different structural modifications, in the frequency range 0 to 500 cm^{-1}. Typical spectra are reproduced on Fig. 1 to 5.

Fig. 1 represents the Raman polarization selections obtained at room temperature (ORT phase) with the Mn and Cd derivatives. These spectra must be examined with caution, because of the existence of twin domains [2, 3, 5, 6]. The domain pattern [2, 6] corresponds to an exchange of the a and c crystallographic axes of the Cmca structure between adjacent domains. This leads to a mixing of the $B_{1g}(\alpha_{xy})$ and $B_{3g}(\alpha_{yz})$ spectra on one hand and of the $A_g(\alpha_{xx})$ and $A_g(\alpha_{zz})$ spectra on the other hand, while the $A_g(\alpha_{yy})$ and $B_{2g}(\alpha_{zx})$ spectra must not be affected by the domain structure. However, additional polarization alteration may occur at the domain boundaries. Anyway, strong scattering from phonons clearly appears for both compounds on the $A_g(\alpha_{yy})$ spectrum, while all other scattering configurations only give rise to very weak and broad features, as indicated on Fig. 1 by the amplification factors. Also, a broad Rayleigh wing is observed on the $A_g(\alpha_{xx}, \alpha_{zz})$ and $B_{2g}(\alpha_{xz})$ spectra; this low-frequency signal is completely absent on all other spectra (Fig. 1).

The spectral evolution observed by varying the temperature through the different structural modifications is shown on Fig. 2 and 3. In the case of $(CH_3NH_3)_2MnCl_4$, a continuous evolution is noticed on the $A_g(\alpha_{yy})$ spectrum of the ORT phase, when increasing the temperature towards the second-order ORT ↔ THT phase transition (Fig. 2a). We observe the progressive disappearance of the Raman peaks at 60 and 120 cm^{-1}, leading to a spectrum $A_{1g}(\alpha_{zz})$ composed of two lines at 130 and 205 cm^{-1} in the THT phase. In the case of $(CH_3NH_3)_2CdCl_4$, this transition occurs at 484 K, i.e. well above the decomposition temperature of the sample. No attempt was made to reach the THT phase without decomposition, by immersion of the sample in silicon oil or grease [6]. No striking evolution of these spectra (Fig. 2a, 3a) can be noticed at the first-order ORT ↔ TLT transition; in contrast, the TLT ↔ MLT phase

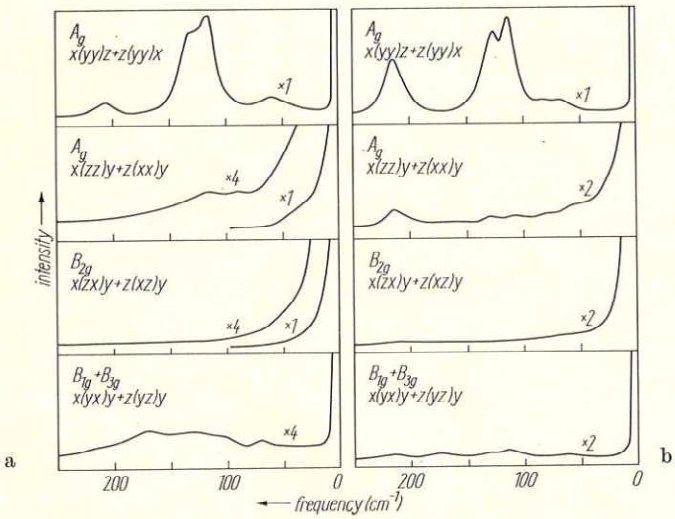

Fig. 1. Polarized low-frequency Raman spectra of a) $(CH_3NH_3)_2MnCl_4$ and b) $(CH_3NH_3)_2CdCl_4$ in the ORT phase at room temperature. The domain pattern of the crystals is taken into account as indicated by notations on the figure, provided the two domain orientations occur with equal probabilities in the crystal samples

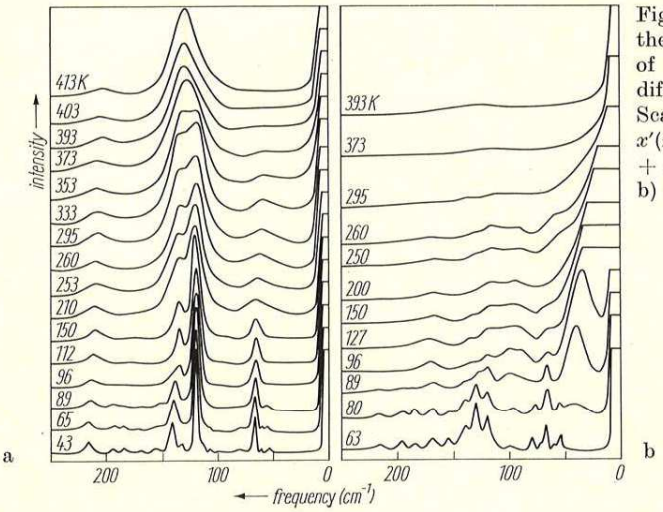

Fig. 2. Temperature evolution of the low-frequency Raman spectra of $(CH_3NH_3)_2MnCl_4$ through the different structural modifications. Scattering geometries: a) THT: $x'(zz)\,y'$ (A_{1g}); ORT: $x(yy)\,z + z(yy)\,x$ (A_g); TLT: $x(zz)\,y$ (A_{1g}). b) ORT: $x(zz)\,y + z(xx)\,y$ (A_g); TLT: $x(yy)\,z$ ($A_{1g} + B_{1g}$)

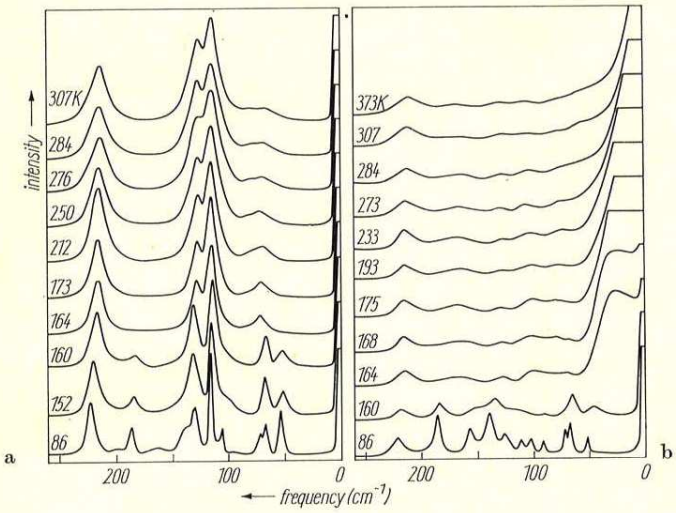

Fig. 3. Temperature evolution of the low-frequency Raman spectra of $(CH_3NH_3)_2CdCl_4$ through the different structural modifications. (The scattering geometries are the same as indicated in Fig. 2)

transformation is well characterized by a sudden narrowing of the spectra as well as by the splitting of several Raman lines and the appearance of new features (Fig. 2a, 3a).

On the weak and broad spectra associated to all other Raman tensor elements, in the frequency range 50 to 250 cm^{-1} no variation can be detected at the ORT $\leftrightarrow$ TLT transition, while the TLT $\leftrightarrow$ MLT transformation is again well characterized (Fig. 2b, 3b). When increasing the temperature close to the THT phase, it is difficult to localize any phonon frequency on these spectra.

In the very low frequency range 0 to 50 cm^{-1}, the above-mentioned Rayleigh wings display a remarkable temperature variation (Fig. 4). This signal is observed only when polarizations of both the incident and scattered lights are parallel to the plane of the $(MCl_4)_n^{2n-}$ layer, i.e. on the $A_g(\alpha_{xx}, \alpha_{zz})$ and $B_{2g}(\alpha_{zx})$ spectra of the ORT phase, and on the $A_{1g} + B_{1g}(\alpha_{xx}, \alpha_{yy})$ and $B_{2g}(\alpha_{xy})$ spectra of the TLT phase. In the

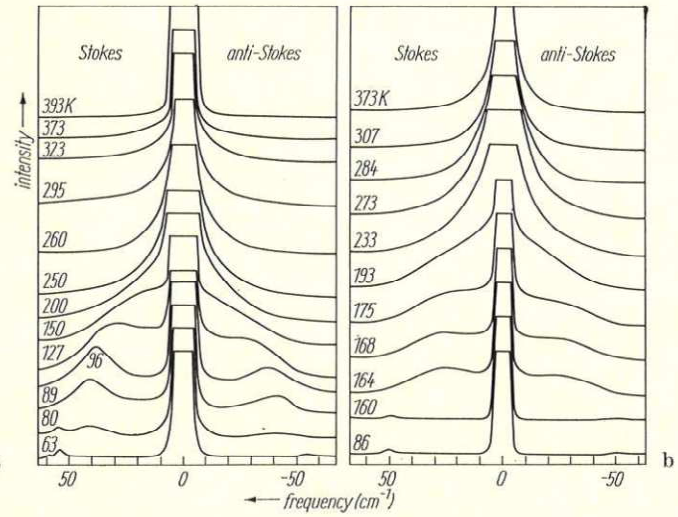

Fig. 4. Detail of the low-frequency (0 to 50 cm^{-1}) response observed in a) $(CH_3NH_3)_2MnCl_4$; b) $(CH_3NH_3)_2CdCl_4$. Scattering geometries: ORT: $x(zz)\,y + z(xx)\,y$ (A_g); TLT: $x(yy)\,z$ ($A_{1g} + B_{1g}$)

ORT phase, this "quasi-elastic" signal progressively decreases and narrows when heating the sample, and can no longer be distinguished from the strong elastic peak at temperatures close to the ORT ↔ THT transition (Fig. 4). Through the ORT ↔ ↔ TLT transition, the signal persists with no striking change of its shape, but we notice an abrupt intensity variation. The intensity ratio is $I(\alpha_{xz})/I(\alpha_{zz}) \approx 1$ in the ORT phase just above the first-order transition and becomes $I(\alpha_{xy})/I(\alpha_{xx}) \approx 0.3$ in the TLT phase, due to a sudden increase of the uncrossed polarization intensity and to a simultaneous decrease of the depolarized part of the "quasielastic" peak. This phenomenon is the unique spectral manifestation of the ORT ↔ TLT transition we could observe. On the other hand, we have performed experiments on crystal samples in the TLT phase, with surfaces perpendicular to the 110 and $\bar{1}10$ directions; again, the signal is observed only on the $A_{1g} + B_{2g}$ $y'(x'x')\,z$ and B_{1g} $y'(x'y')\,z$ spectra, but now the intensity ratio is $I(\alpha_{x'x'})/I(\alpha_{x'y'}) \approx 0.3$, thus showing there is no A_{1g} component. Then, in the TLT phase, the "quasielastic" peak corresponds to the B_{1g} and B_{2g} representations of the D_{4h} point group.

When cooling the sample in the TLT phase, the Rayleigh wings broaden and then can be clearly separated from the elastically scattered light, giving rise to a well-defined maximum at ≈ 30 cm^{-1} in $(CH_3NH_3)_2CdCl_4$, and at ≈ 40 cm^{-1} in $(CH_3NH_3)_2 \cdot \cdot MnCl_4$, just above the transition temperature to the MLT phase (Fig. 4). Furthermore, there is a sudden disappearance of this signal when going into the MLT phase (Fig. 2 to 4). These results complement a previous observation by Dultz [17] on $(CH_3NH_3)_2 \cdot \cdot MnCl_4$.

Finally, we have also performed some measurements in the frequency range 250 to 500 cm^{-1} with $(CH_3NH_3)_2CdCl_4$ crystals. Two very weak features at 450 and 335 cm^{-1} can be localized in the MLT phase (Fig. 5). The 450 cm^{-1} Raman line disappears just below the MLT ↔ TLT transition temperature, while at this transition the 335 cm^{-1} peak is shifted abruptly to 295 cm^{-1} and then broadens continuously when heating the sample through the TLT and ORT phases (Fig. 5). It is interesting to notice that this line presents the same polarization selections as the low-frequency "quasielastic" peak.

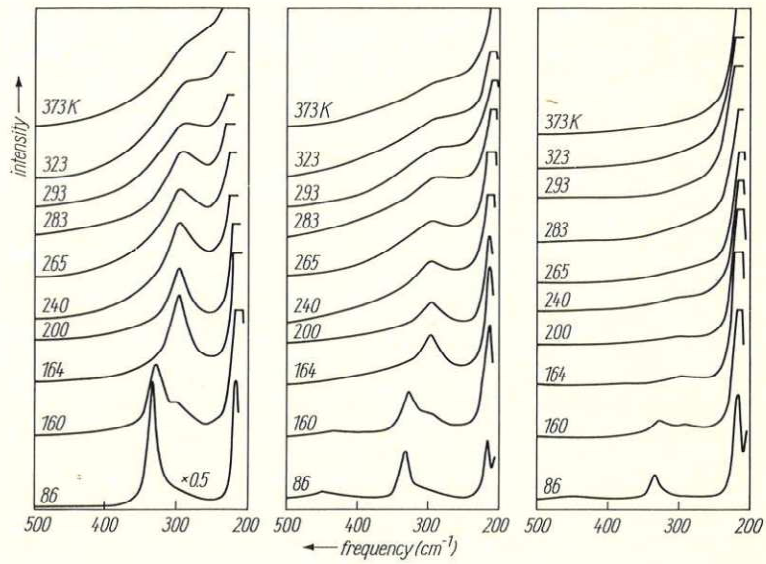

Fig. 5. Polarized Raman spectra of $(CH_3NH_3)_2CdCl_4$ in the 200 to 500 cm^{-1} frequency range. Scattering geometries: a) ORT: $x(zz)\,y + z(xx)\,y$ (A_g); TLT: $x(yy)\,z$ ($A_{1g} + B_{1g}$). b) ORT: $x(zx)\,y + z(xz)\,y$ (B_{2g}); TLT: $x(yx)\,z$ (B_{2g}). c) ORT: $x(yx)\,y + z(xz)\,y$ ($B_{1g} + B_{3g}$); TLT: $x(zx)\,z$ (E_g)

5. Discussion

5.1 Assignment of the spectra

A detailed assignment of these spectra is not obvious because of the great number of Raman-active lattice vibrations (Table 1). Furthermore, additional difficulties arise from the possibility of a breakdown of the $K = 0$ selection rules in the orientationally disordered phases [21], and also by crystal twinning in the ORT and MLT phases [2 to 6].

There is, however, the favourable case of the $A_{1g}(\alpha_{zz})$ spectrum in the THT phase (Fig. 2a), where only two peaks are observed in agreement with group-theoretical predictions for the time-averaged structure (Table 1). The eigenvectors of these lattice vibrations correspond to a linear combination of antiparallel displacements of the Cl(2) axial atoms and of the $CH_3NH_3^+$ groups as a whole in the Z-direction [19]. When comparing this spectrum of $(CH_3NH_3)_2MnCl_4$ (Fig. 2a) with that of $(C_2H_5NH_3)_2 \cdot MnCl_4$ [18] at 425 K in the THT phase [12], the Raman line at 205 cm^{-1} remains approximately at the same frequency while that at 130 cm^{-1} is shifted to 105 cm^{-1} in the ethyl compound, i.e. according to the square root of the reduced-mass ratio of the molecular cations. Thus, the 205 cm^{-1} peak is essentially due to the axial Mn–Cl(2) stretching vibration, and the 130 and 105 cm^{-1} lines correspond to the translational vibration of the $CH_3NH_3^+$ and the $C_2H_5NH_3^+$ cations parallel to the unique Z-axis, respectively. In this case, the separation of the lattice vibration we have made in Table 1 is correct. The new features appearing on the $A_g(\alpha_{yy})$ spectrum in the ORT phase must come from the $\tau_5(B_{3g})$ zone boundary phonons at point X of the THT Brillouin zone [19]. Only two of them can be distinguished on the $A_g(\alpha_{yy})$ spectrum at ≈ 60 and 118 cm^{-1} with $(CH_3NH_3)_2MnCl_4$ (Fig. 2a) among the four expected ones [19].

Similarly, we can assign the ORT phase $A_g(\alpha_{yy})$ spectrum of $(CH_3NH_3)_2CdCl_4$ (Fig. 3a): the line at 213 cm^{-1} must be due to the axial CdCl(2) stretching vibration, that at 136 cm^{-1} to the translational vibration of the $CH_3NH_3^+$ groups, and the frequencies at 65, 80, and 114 cm^{-1} come from the $\tau_5(B_{3g})$ modes at point X of the THT Brillouin zone.

The same interpretation can also be extended to the $A_{1g}(\alpha_{zz})$ spectrum of the TLT phase (Fig. 2a, 3a), since no further phonon mode is observed according to our group-theoretical arguments for the totally symmetric representation (Table 1). In the MLT phase, polarization selections are altered in part by crystal misalignment due to the slight tilting of crystallographic axes at the TLT $\leftrightarrow$ MLT transition, and also by the domain structure of this phase [6]. However, one can always qualitatively situate the M–Cl(2) stretching vibration and the $CH_3NH_3^+$ translatory mode at 215 to 200 and 140 to 130 cm^{-1}, respectively (Fig. 2a, 3a).

No precise assignment can be proposed for the weak and broad spectra obtained for all other Raman tensor elements (Fig. 1). It is often difficult to decide if the observed features really correspond to the considered tensor element, or if they are due to an orientational spill-over of scattering from the strong $A_g(\alpha_{yy})$ and $A_{1g}(\alpha_{zz})$ phonon modes in the ORT and TLT phases, respectively. Furthermore, only a few modes can be distinguished among the expected ones, especially in the TLT phase (Table 1). Nevertheless, the very weak line observed at 450 cm^{-1} in the MLT phase of $(CH_3NH_3)_2CdCl_4$ (Fig. 5) could be assigned to the ν_6 torsional oscillation of the $CH_3NH_3^+$ cation, since it was localized at about 470 cm^{-1} in the case of CH_3NH_3Cl in its low-temperature modification [22 to 25]. It is also tempting to assign the line at 290 to 335 cm^{-1} (Fig. 5) to the librational mode of the cation around its molecular axis, by analogy with CH_3NH_3Cl, where it was observed at $\approx$ 270 cm^{-1} [24, 25]. Indeed, it is shifted to $\approx$ 250 cm^{-1} in $(C_2H_5NH_3)_2CdCl_4$ [26], thus providing it is essentially a "cationic" vibration. In CH_3NH_3Cl some coupling occurs between this libration and the ν_6 torsional oscillation [22, 25, 27]. Such a coupling might also occur in $(CH_3NH_3)_2 \cdot CdCl_4$. Nevertheless, for simplication, we shall call "R_z libration" the vibrational mode at 290 cm^{-1}, knowing it is not necessarily the exact description of the normal vibration. The study of deuterated samples is necessary in order to go further in the analysis of the librational modes [25].

5.2 Analysis of the phase sequence

The strong analogy between the low-frequency Raman spectra of $(CH_3NH_3)_2MnCl_4$ and $(CH_3NH_3)_2CdCl_4$ through their different structural modifications confirms that structure and phase sequence are very similar in these two compounds [3 to 6].

Following previous NMR results [6 to 10], the three high-temperature (THT, ORT, and TLT) phases display some kind of dynamical disorder with respect to the orientation of the $CH_3NH_3^+$ cations. Indeed, the corresponding low-frequency Raman spectra always exhibit broad features, in contrast with the MLT ordered phase. Furthermore, the existence of disorder in the ORT and TLT phases is evidenced by a breakdown of the $K = 0$ selection rules derived from idealized ordered structures (Table 1). As already pointed out the librational mode R_z of the cation about its long axis is observed at about 300 cm^{-1} (Fig. 5) only when polarization of both the incident and the scattered light is set parallel to the plane of the layer, i.e. on the $A_g(\alpha_{xx}, \alpha_{zz})$ and the $B_{2g}(\alpha_{zx})$ spectra of the ORT phase and on the $B_{1g}(\alpha_{xx}, \alpha_{yy})$ and $B_{2g}(\alpha_{xy})$ spectra of the TLT phase. Now, it is evident from Table 2 there must be no A_g and no B_{2g} component of this R_z mode in the ORT and TLT phase, respectively, if we assume the cation to be ordered; furthermore, there is no domain structure in the TLT phase which could cause this phenomenon. Thus, the C_s site symmetry of the $CH_3NH_3^+$

Similarly, we can assign the ORT phase $A_g(\alpha_{yy})$ spectrum of $(CH_3NH_3)_2CdCl_4$ (Fig. 3a): the line at 213 cm^{-1} must be due to the axial CdCl(2) stretching vibration, that at 136 cm^{-1} to the translational vibration of the $CH_3NH_3^+$ groups, and the frequencies at 65, 80, and 114 cm^{-1} come from the $\tau_5(B_{3g})$ modes at point X of the THT Brillouin zone.

The same interpretation can also be extended to the $A_{1g}(\alpha_{zz})$ spectrum of the TLT phase (Fig. 2a, 3a), since no further phonon mode is observed according to our group-theoretical arguments for the totally symmetric representation (Table 1). In the MLT phase, polarization selections are altered in part by crystal misalignment due to the slight tilting of crystallographic axes at the TLT $\leftrightarrow$ MLT transition, and also by the domain structure of this phase [6]. However, one can always qualitatively situate the M–Cl(2) stretching vibration and the $CH_3NH_3^+$ translatory mode at 215 to 200 and 140 to 130 cm^{-1}, respectively (Fig. 2a, 3a).

No precise assignment can be proposed for the weak and broad spectra obtained for all other Raman tensor elements (Fig. 1). It is often difficult to decide if the observed features really correspond to the considered tensor element, or if they are due to an orientational spill-over of scattering from the strong $A_g(\alpha_{yy})$ and $A_{1g}(\alpha_{zz})$ phonon modes in the ORT and TLT phases, respectively. Furthermore, only a few modes can be distinguished among the expected ones, especially in the TLT phase (Table 1). Nevertheless, the very weak line observed at 450 cm^{-1} in the MLT phase of $(CH_3NH_3)_2CdCl_4$ (Fig. 5) could be assigned to the ν_6 torsional oscillation of the $CH_3NH_3^+$ cation, since it was localized at about 470 cm^{-1} in the case of CH_3NH_3Cl in its low-temperature modification [22 to 25]. It is also tempting to assign the line at 290 to 335 cm^{-1} (Fig. 5) to the librational mode of the cation around its molecular axis, by analogy with CH_3NH_3Cl, where it was observed at $\approx$ 270 cm^{-1} [24, 25]. Indeed, it is shifted to $\approx$ 250 cm^{-1} in $(C_2H_5NH_3)_2CdCl_4$ [26], thus providing it is essentially a "cationic" vibration. In CH_3NH_3Cl some coupling occurs between this libration and the ν_6 torsional oscillation [22, 25, 27]. Such a coupling might also occur in $(CH_3NH_3)_2 \cdot CdCl_4$. Nevertheless, for simplication, we shall call "R_z libration" the vibrational mode at 290 cm^{-1}, knowing it is not necessarily the exact description of the normal vibration. The study of deuterated samples is necessary in order to go further in the analysis of the librational modes [25].

5.2 Analysis of the phase sequence

The strong analogy between the low-frequency Raman spectra of $(CH_3NH_3)_2MnCl_4$ and $(CH_3NH_3)_2CdCl_4$ through their different structural modifications confirms that structure and phase sequence are very similar in these two compounds [3 to 6].

Following previous NMR results [6 to 10], the three high-temperature (THT, ORT, and TLT) phases display some kind of dynamical disorder with respect to the orientation of the $CH_3NH_3^+$ cations. Indeed, the corresponding low-frequency Raman spectra always exhibit broad features, in contrast with the MLT ordered phase. Furthermore, the existence of disorder in the ORT and TLT phases is evidenced by a breakdown of the $K = 0$ selection rules derived from idealized ordered structures (Table 1). As already pointed out the librational mode R_z of the cation about its long axis is observed at about 300 cm^{-1} (Fig. 5) only when polarization of both the incident and the scattered light is set parallel to the plane of the layer, i.e. on the $A_g(\alpha_{xx}, \alpha_{zz})$ and the $B_{2g}(\alpha_{zx})$ spectra of the ORT phase and on the $B_{1g}(\alpha_{xx}, \alpha_{yy})$ and $B_{2g}(\alpha_{xy})$ spectra of the TLT phase. Now, it is evident from Table 2 there must be no A_g and no B_{2g} component of this R_z mode in the ORT and TLT phase, respectively, if we assume the cation to be ordered; furthermore, there is no domain structure in the TLT phase which could cause this phenomenon. Thus, the C_s site symmetry of the $CH_3NH_3^+$

ORT and TLT phases (Fig. 4), as well as on those of the ethyl compounds $(C_2H_5NH_3)_2 \cdot MCl_4$ (M = Mn, Cd) in their room temperature modification [26]. At temperatures just above the TLT ↔ MLT transition, it looks like a damped-oscillator response, whose frequency and/or damping constant decreases and increases when heating the sample in the TLT and ORT phases, respectively, giving rise progressively to an overdamped oscillator or a relaxation-like response (Fig. 4). There is a sudden disappearance of this signal in the MLT phase (Fig. 4) where it is probably replaced by an underdamped phonon mode in the 50 to 80 cm^{-1} frequency range (Fig. 2 and 3). A detailed study of the temperature variation of the soft-mode parameters will be presented in a forthcoming paper.

The reorientational motions of the $CH_3NH_3^+$ cation as a whole (i.e. the tumbling mode of the CN bond) as well as the hindered rotations of the NH_3 and CH_3 groups are closely related to the mechanism for the phase sequence, and then must be somehow associated with the observed soft-mode behaviour [19]. Indeed, as already pointed out, the soft-mode exhibits the same polarization selections as the R_z librational mode, which is the vibrational counterpart of the reorientational motion of the cation. On the other hand, as shown by NMR results [8, 9], these reorientational motions probably lie in the microwave region of 10^9 to 10^{11} s^{-1} [19], i.e. well below the frequency range of the observed soft mode: this is in agreement with the presence on the spectra of the R_z libration even at high temperatures (Fig. 5), whereas it could no longer exist as a resonant mode if very fast reorientation or free rotation occur. Then, we may conclude the observed soft-mode behaviour comes from some coupling of particular phonons with the hydrogen relaxational motion.

In the ORT phase, the eigenvectors of the soft mode represent a linear combination of the A_g symmetry vectors, and can be reasonably approximated by a "rotation" of the MCl_6 octahedra and of the $CH_3NH_3^+$ groups around the a-axis [19]. This latter (R_x libration) must be seen as a tilting of the time-averaged C–N direction caused by a biasing of the $CH_3NH_3^+$ tumbling mode [9]. An estimate of the relative contribution of these motions to the soft-mode eigenvectors is difficult; further elements for the discussion could be given by the study of deuterated samples. However, the observation in the THT phase of four tilted configurations of the MCl_6 octahedra correlated to the four different orientations of the $CH_3NH_3^+$ cations [3], supports the possibility of a coupling of the MCl_6 "rotational" mode with reorientational motions of the cations. Such a coupling with the disordering mode could explain the observed breakdown in the $K = 0$ selection rules for both the R_z libration and the soft mode.

No explanation by means of a soft-mode picture is possible for the first-order ORT ↔ TLT and TLT ↔ MLT transitions [6]. Then, the presence of a soft-mode behaviour in the TLT phase cannot be related to the occurrence of neither the ORT nor the MLT transition: indeed, the observed signal does not soften but has a strong tendency to harden close to the MLT transition temperature and seems to go through the OTR ↔ TLT transition without any striking modification (Fig. 4). A possibility — but not necessarily the unique one — is to consider it is a "symmetry restoring" mode of the THT high-temperature phase, associated to an hypothetical TLT ↔ THT transition, which cannot occur because of the appearance of the ORT phase as an intermediate state. Thus, the variation in the relative intensities of the polarized and depolarized components of the soft mode observed at the ORT ↔ TLT transition may be the result of the biasing of the tumbling mode, leading to a different distribution of the $CH_3NH_3^+$ occupation probabilities in the potential wells, according to model (i) or model (iii) [10]. However, the possibility of an experimental artefact due to the disappearance of the domain structure of the crystal in the TLT phase [2] cannot be completely ruled out.

We have to emphasize the above discussion on soft-mode behaviour in the ORT and TLT phases is just speculative, and must be considered as starting hypothesis for further investigations; in particular, the study of deuterated samples and the knowledge of the temperature evolution of the soft-mode parameters will give mode precise elements for the discussion.

Acknowledgements

The authors wish to thank Dr. H. Arend and Dr. R. Kind (E. T. H. Zürich) for helpful discussions and for providing their results prior to publication. It is also a pleasure to thank Mr. R. Cavagnat and Mr. J. C. Cornut for valuable experimental help.

References

[1] E. R. Peterson and R. D. Willett, J. chem. Phys. **56**, 1879 (1972).
[2] K. Knorr, I. R. Jahn, and G. Heger, Solid State Commun. **15**, 231 (1974).
[3] G. Heger, D. Mullen, and K. Knorr, phys. stat. sol. (a) **31**, 455 (1975).
[4] G. Heger, D. Mullen, and K. Knorr, phys. stat. sol. (a) **35**, 627 (1976).
[5] G. Chapuis, H. Arend, and R. Kind, phys. stat. sol. (a) **31**, 449 (1975).
[6] G. Chapuis, R. Kind, and H. Arend, phys. stat. sol. (a) **36**, 285 (1976).
[7] D. Brinkmann, U. Walther, and H. Arend, Solid State Commun. **18**, 1307 (1976).
[8] R. Blinc, M. Burgar, B. Lozar, J. Seliger, J. Slak, V. Rutar, H. Arend, and R. Kind, J. chem. Phys. **66**, 278 (1977).
[9] R. Kind and J. Roos, Phys. Rev. B **13**, 45 (1976).
[10] J. Seliger, R. Blinc, R. Kind, and H. Arend, Z. Phys. **25B**, 189 (1976).
[11] A. Levstik, C. Filipic, R. Blinc, H. Arend, and R. Kind, Solid State Commun. **20**, 127 (1976).
[12] H. Arend, R. Hofmann, and F. Waldner, Solid State Commun. **13**, 1629 (1973).
[13] E. H. Bocanegra, M. J. Tello, M. A. Arrandiaga, and H. Arend, Solid State Commun. **17**, 1221 (1975).
[14] N. Lehner, K. Strobel, R. Geick, and G. Heger, J. Phys. C 8, 4096 (1975).
[15] J. H. M. Stoelinga and P. Wyder, J. chem. Phys. **64**, 4612 (1976).
[16] I. A. Oxton and O. Knop, J. Mol. Structure **37**, 59 (1977).
[17] W. Dultz, in: Molecular Spectroscopy of Dense Phases, Proc. XII. E.C.M.S., Strasbourg 1975, Elsevier Publ. Co., Amsterdam 1976 (p. 211).
[18] A. Daoud, Thesis, Dijon 1976.
[19] J. Petzelt, J. Phys. Chem. Solids **36**, 1005 (1975).
[20] R. Cavagnat, J. C. Cornut, M. Couzi, and G. Daleau, Analusis, in the press.
[21] E. Whalley and J. E. Bertie, J. chem. Phys. **46**, 1264 (1967).
[22] A. Theoret and C. Sandorfy, Spectrochim. Acta **23A**, 519 (1967).
[23] E. Castellucci, J. Mol. Structure **23**, 449 (1974).
[24] S. Forss, N. Meinander, and F. Stenman, Proc. V. Internat. Conf. Raman Spectroscopy, Freiburg 1976 (p. 556).
[25] C. J. Ludman, C. I. Ratcliffe, and T. C. Waddington, J. Chem. Soc., Faraday Trans. II **72**, 1759 (1976).
[26] M. Couzi, unpublished results.
[27] J. Tegenfeldt, J. Phys. Chem. Solids **33**, 215 (1972).

(Received March 8, 1977)